Journal of Southeast University (English Edition) Vol. 25, No. 4, pp. 439 – 444 Dec. 2009 ISSN 1003—7985

Modeling for Ethernet passive optical network receiver

Zhang Liang Wang Zhigong Hu Qingsheng Deng Weijie

(Institute of RF- & OE-ICs, Southeast University, Nanjing 210096, China)

Abstract: A behavior model for the receiver of the Ethernet passive optical network (EPON) is presented. The model consists of a fiber, a photodetector, a transimpedance amplifier (TIA) followed by a limiting amplifier and a clock and data recovery circuit (CDR). Each sub-model is constructed based on the architecture of a circuit. The noise and jitter in each block such as shot noise, thermal noise, deterministic and random jitter are also considered. The performance of the whole receiver can be evaluated by the simulation of the behavior model, which is faster than the ordinary circuit model and more accurate than the analytical model. The whole model is implemented with C++ and simulated in Microsoft Visual C++ 6.0. Using the Monte Carlo method, the EPON receiver is simulated. The simulation results show a good agreement with experimental ones.

Key words: Ethernet passive optical network (EPON); behavior model; noise; jitter; clock and data recovery circuit (CDR)

The Ethernet passive optical network (EPON) integrates Ethernet access technology and a broadband PON system to provide a high-speed and long-distance access application for Ethernet. The EPON has many advantages such as high bandwidth, cost effectiveness, easy management and maintainability. With the rapid development of the EPON, especially the high speed EPON, it is essential to model and analyze the EPON system with the aim of increasing the bit rate and reducing the overall cost.

Generally, the methods of modeling and analyzing a communication system fall into three categories: those based on analytical calculations, those based on time-domain Monte Carlo simulations, and hybrid approaches based on a combination of simulations and analytical calculations. With the increase in bit rate, it is increasingly important to consider noise effects on the EPON performance. There are several commercial products which permit users to simulate optical communication systems; however, they use simplified circuit models which cannot analyze noise effects in detail or are too complex to simulate within an acceptable time[1-4]. Furthermore, no current mature tools can simulate a whole optical communication system.

Because of the complexity of the laser diode, the transmitter of the EPON is not included in this paper. An accurate and fast simulator based on C++ for the EPON receiver is proposed. All components used in the EPON receiver such as fiber, photodiode, transimpedance amplifier (TIA), limiting amplifier (LA) and clock and data recovery circuits (CDR) are researched. Using the proposed simulator, both optical device and system designers can simulate a complete EPON system and evaluate its performance before design and implementation.

Received 2009-06-02.

Biographies: Zhang Liang (1982—), male, graduate; Wang Zhigong (corresponding author), male, doctor, professor, zgwang@seu.edu.cn.

Citation: Zhang Liang, Wang Zhigong, Hu Qingsheng, et al. Modeling for Ethernet passive optical network receiver[J]. Journal of Southeast University (English Edition), 2009, 25(4): 439 – 444.

1 Receiver Architecture of EPON

As shown in Fig. 1, an EPON receiver consists of five blocks: an optical fiber, a photodetector, a TIA, an LA and a CDR. To simulate the receiver performance, a generator and an analyzer are used to generate a set of sampling data and analyze the responses. For modeling a whole EPON receiver, each function block used in the system is modeled as accurately as possible based on its function. Various factors affecting the receiver performance are considered. For example, when modeling the optical fiber, factors resulting in the signal degradation are researched, while in other function blocks, noises and jitters such as shot noise, thermal noise, deterministic and random jitter are investigated. On the other hand, this simulator can also give multiple result shapes, such as signal waveforms, eye diagrams, deterministic and random jitter, and bit error ratio (BER).

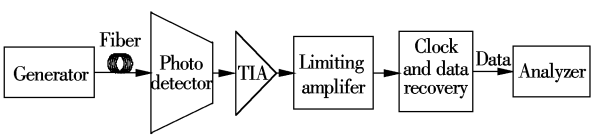

Fig. 1 The block diagram of EPON receiver

1.1 Modeling for fiber link

A fiber link can be considered as a low-pass filter, in which fiber attenuation and pulse-width extension resulting from dispersion are taken into account.

Let A_{tt} be the fiber attenuation, and it can be expressed as

$$A_{tt} = 10\log \frac{P_{out}}{P_{in}} \tag{1}$$

where P_{out} is the output power of the fiber and P_{in} is the input power. In the simulator, A_{tt} is a given parameter based on the practical optical fiber.

Suppose that T_{out} and T_{in} are the width of optical pulses for the output and input optical signals, respectively. And ΔT is the broadened width of optical pulses. The pulse-width extension of optical pulses is shown as

$$T_{out} = (T_{in}^2 + \Delta T^2)^{1/2} \tag{2}$$

Let L be the fiber length, D be the dispersion parameter (unit ps/(km · nm)), $\Delta\lambda$ be the linewidth (full width at half maximum) of the laser. Then $\Delta T = LD\Delta\lambda$.

In this simulator, the pulse width extension is modeled in time domain by changing the sampling value of the waveform. After determining the sign of the incremental value which is according to the slope of the waveform, the broadening factor is computed using the trigonometric method. Then, the output waveform is obtained by changing the sam-

pling value.

1.2 Modeling for photodetector

PIN(positive intrinsic negative) and APD(avalanche photodiode) are two kinds of photodiodes used in the EPON. The fundamental difference is that a PIN does not have an internal gain, while an APD has an internal gain due to its self-multiplication.

Supposing that P_{in} is the input signal power, then the average signal current of a PIN is

$$i_s = RP_{in} \tag{3}$$

where R is the responsivity of the photodetector(unit A/W) and can be expressed as

$$R = \frac{\eta q}{h\nu} \approx \frac{\eta \lambda}{1.24} \tag{4}$$

where η is the quantum efficiency; q is the electron charge; h is the Planck constant; ν and λ are the velocity of light and the wavelength of the signal, respectively.

Since an APD photodiode is biased into the avalanche region, it has a gain of electrons produced in the avalanche. Let G stand for the average gain. We can obtain the average signal current of the APD as follows:

$$i_s = GRP_{in} \tag{5}$$

The total current of a photodiode is the sum of i_s and i_d, which is the dark current,

$$i_{s+d}(t) = i_s(t) + i_d(t) \tag{6}$$

On the other hand, shot noise and thermal noise are two fundamental noise sources contributing to the current fluctuation. Shot noise results from the corpuscular nature of transport and can be assumed as a stationary random process with Poisson statistics. However, it is generally approximated by Gaussian statistics. Supposing that B is the bandwidth, for a PIN receiver, its shot noise is

$$\overline{i_{shot}^2} = 2Bqi_{s+d}(t) \tag{7}$$

While for an APD receiver, considering its excess noise factor of F, its shot noise can be expressed as[4]

$$\overline{i_{shot}^2} = 2FGBqi_{s+d}(t) \tag{8}$$

where

$$F = k_A G + (1 - K_A)\left(2 - \frac{1}{G}\right) \tag{9}$$

and k_A is the ionization-coefficient ratio.

Meanwhile, thermal noise is caused by the load of the optical receiver and can be analyzed using Gaussian statistics, that is

$$i_T^2 = \frac{4kTB}{R} \tag{10}$$

where k is the Boltzmann constant and T is the absolute temperature.

In practical use, the performance of a photodetector is often evaluated by carrier-to-noise ratios(CNRs) using the following equations:

$$\mathrm{CNR}_{PIN} = \frac{i_s^2}{\overline{i_{shot}^2} + \overline{i_T^2}} = \frac{(RP_{in})^2}{2Bqi_{s+d}(t) + 4kTB/R} \tag{11}$$

$$\mathrm{CNR}_{APD} = \frac{i_s^2}{\overline{i_{shot}^2} + \overline{i_T^2}} = \frac{(GRP_{in})^2}{2FGBqi_{s+d}(t) + 4kTB/R} \tag{12}$$

For simulating the PIN and the APD in this simulator, first Gaussian noise is generated, and then the mean and variance of Gaussian noise are calculated according to Eqs. (7), (8) and(10). After that, the output current is calculated according to Eqs. (3), (5) and (6). Finally, CNRs are obtained based on Eqs. (11) and (12).

1.3 Modeling for TIA

The function of the TIA is to transform a current signal from a photodiode into a voltage signal and then amplify it. While the LA converts the output swing of the TIA to a sufficient logic level for the CDR. Generally, the TIA circuit can be regarded as a digital filter with the parameters derived from the transfer function of a real TIA circuit[5]. Fig. 2 is the equivalent circuit of the TIA, in which the transimpedance stage consists of an inverting amplifier with a feedback resistor of R_f. We can obtain its transform function $H(s)$ as follows:

$$H(s) = \frac{V_o}{I_s} = \frac{B}{S + \tau} \tag{13}$$

where B is the bandwidth of the TIA, $B = A_v/C_T$; $\tau = (1 - A_v)/(C_T R_f) + 1/(R_T C_T)$. A_v is the gain of the amplifier; C_T is the output capacitance of the photodiode; R_T is the input impedance of the amplifier.

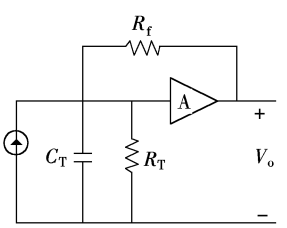

Fig. 2 Equivalent circuit of transimpedance amplifier

Using the bilinear transformation method, $H(z)$ can be expressed as

$$H(z) = \frac{V(z)}{I_s(z)} = \frac{B(1 + z^{-1})}{2f_s(1 - z^{-1}) + \tau(1 + z^{-1})} \tag{14}$$

where f_s is the sampling frequency.

From Eq. (14), we can obtain the relationship between input and output as shown below:

$$v(n) = Dv(n-1) + E[i_s(n) + i_s(n-1)] \tag{15}$$

where $D = (2f_s - \tau)/(2f_s + \tau)$ and $E = B/(2f_s + \tau)$.

Thus, the output voltage V of the TIA can be calculated based on the output current of the photodetector.

1.4 Modeling for LA

The LA provides an additional voltage gain for the signal to satisfy the input sensitivity of the attached clock and data recovery circuit. The LA is a typical nonlinear amplifier. The Cann model[6] is adopted for the modeling of the LA, which is one of the most popular models for nonlinear amplifiers. The Cann model can permit independent control of the gain, the limiting value, and the sharpness of the transition characteristic. The expression of the Cann model can be written as

$$v_o = \frac{g v_{in}}{\left[1 + \left(\frac{g}{L} | v_{in} |\right)^S\right]^{1/S}} \tag{16}$$

where g is the small-signal gain; L is the limit value of the output signal; and s controls the sharpness of the transition from a linear to a limiting state.

The coefficients in Eq. (16) can be obtained by using the curve fitting method, and the accuracy of the Cann model is dependent on the order of curve fitting. An order of 23 is selected as a tradeoff between accuracy and computational cost.

1.5 Modeling for CDR

Generally, the CDR consists of three modules: a phase detector(PD), a charge pump low pass filter(LPF), and a voltage controlled oscillator(VCO), as shown in Fig. 3. In a PLL-based CDR, the PD is used to lock the VCO output signal to the reference clock. Normally, the reference clock is a sub-multiple of the bit rate. Therefore, a divided down version of the VCO clock is used for the comparison. Once the VCO is locked to the approximate bit-rate frequency defined by the reference clock, the logic circuit switches the VCO correction values to the inputs of the delay line phase-frequency detector, which further adjusts the VCO to match the exact frequency of the received data rate. Then the retimer determines the input data based on the VCO output signal.

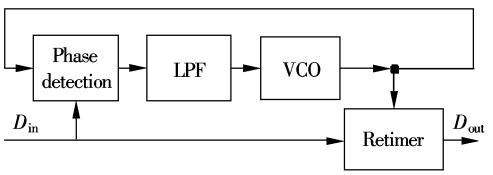

Fig. 3 Block diagram of CDR

In our simulator, a 3-state detector is used as a phase and frequency detector(PFD) because it is simple for simulation[7]. As shown in Fig. 4, state −1, state 0 and state 1 are the states in which the clock frequencies are higher than, equal to and lower than the frequency of D_{in}, respectively. State 0 is the assumed initial state(both U_p and D_n are zero). Then when a rising edge of "fb" occurs, both U_p and D_n are high for an instant. The maximum useful frequency for this PD is limited by the minimum duration of state 0. The PD is not sensitive to the duty cycle of the VCO or the reference oscillator.

The loop filter used in this simulator is a passive-lag loop filter. Fig. 5 depicts the used loop filter. Then if τ_2 is much smaller than τ_1, the transfer function $H(s)$ can be expressed

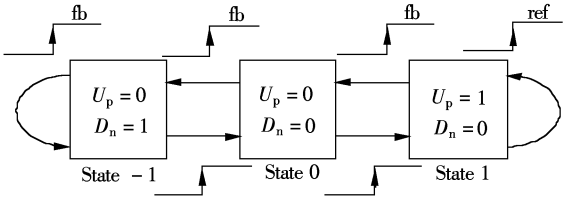

Fig. 4 State transfer diagram of PD

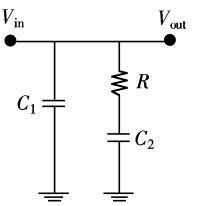

Fig. 5 Low pass filter

by the following approximation:

$$H(s) = \frac{1 + sRC_2}{s^2 RC_1 C_2 + s(C_1 + C_2)} \tag{17}$$

Considering the nonlinear effect of the voltage-controlled curve, an accurate VCO can be modeled as

$$f_{out} = f_c + K_1 V_c + K_2 V_c^2 + K_3 V_c^3 \tag{18}$$

where f_c is the central frequency of the oscillator; V_c is the output voltage generated by the LPF; K_1, K_2, K_3 are the coefficients which can be obtained by the voltage-controlled curve in the device's datasheet.

2 Noises and Jitters

Receiver noise arises from a variety of sources, such as electronic circuit noise, shot noise and avalanche multiplication noise. The latter two kinds of noise have been discussed in section 1.2. In this section, electronic circuit noise mainly appearing in the TIA, LA and CDR is discussed. This kind of noise can be assumed as a zero-mean Gaussian random process with a variance determined by the average power of equivalent input noise. The random generator for the Gaussian random process can be described by the Box-Muller algorithm[8]:

$$X = [-2\ln(U_1)]^{1/2} \cos(2\pi U_2) \tag{19}$$

where U_1 and U_2 are two random numbers from the continuous uniform distribution.

Based on the noise model discussed above, we can add the noise to the sampling signals in order to evaluate its effect on system performance. For example, in Fig. 3, the noise of the PD and the VCO are dominant. The output of the PD is a voltage signal; therefore, a voltage noise is superimposed on the output voltage. The output of the VCO is in the phase domain and contributes to the phase error, so the noise is added on to the phase of the VCO. The RMS value of the noise can be obtained by the simulation of detailed circuits.

On the other hand, timing jitters have significant effects on the performance of the whole system. Jitters can be divided into two categories: deterministic jitter(DJ) and random jitter(RJ). DJ is bounded peak-to-peak and does not have a Gaussian distribution. RJ is considered unbounded and a

Gaussian process in nature. So in the proposed simulator, jitter is modeled as random Gaussian data for the peaks; meanwhile, for the value between peaks, it is modeled as bounded random data. Fig. 6 shows the histogram of the generated jitter.

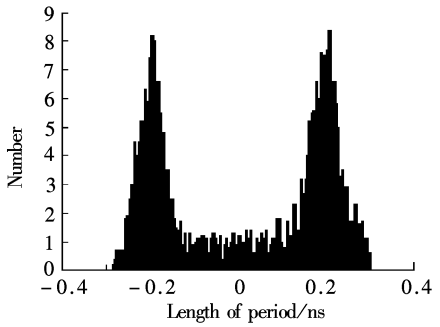

Fig. 6 The histogram of generated jitter

3 Simulation Results

The whole model is implemented with C++ and simulated in Microsoft Visual C++ 6.0. Using the Monte Carlo method, an EPON receiver is simulated and the typical simulation parameters are shown in Tab. 1. These parameters can be categorized into four types:

1) Those used for the fiber link;
2) Those used for the photodetector;
3) Those used for the TIA and LA;
4) Those used for the CDR.

Except for the first type of parameters which can be set based on the EPON standards, all the other parameters can be set based on the datasheet of corresponding devices.

Tab. 1 Simulation parameters

Type	Parameters	Typical value
1	Bandwidth/GHz	8
	Optical power/dBm	−14
	Attenuation/(dB · km^{-1})	0.4
	Dispersion/(s · (nm · km)$^{-1}$)	6.42×10^{-12}
	Fiber length/km	10
2	Responsivity	0.8
	Dark current/nA	100
	Quantum efficiency/%	59
	Average gain of APD	9
	Ionization-coefficient ratio	0.035 or 0.6
3	Input noise voltage of TIA/μV	1.62
	Deterministic jitter of TIA/ps	10.7
	Random jitter of TIA/ps	0
	Input noise voltage of LA/μV	2
	Deterministic jitter of LA/ps	16
	Random jitter of LA/ps	1.1
4	Frequency of reference clock/GHz	9.6
	VCO gain/(MHz · V^{-1})	100
	Capacitor in the loop filter/pF	0.1
	Resistor in the loop filter/Ω	314
	Charge current/μA	10

Figs. 7 to 9 show end-to-end simulation results for the whole receiver. From the figures, a fast evaluation on the feasibility of the design can be obtained.

Fig. 10 shows the BER simulation results for the APD and PIN receivers. Obviously, it can be seen that the APD outperforms the PIN due to the internal gain of the APD.

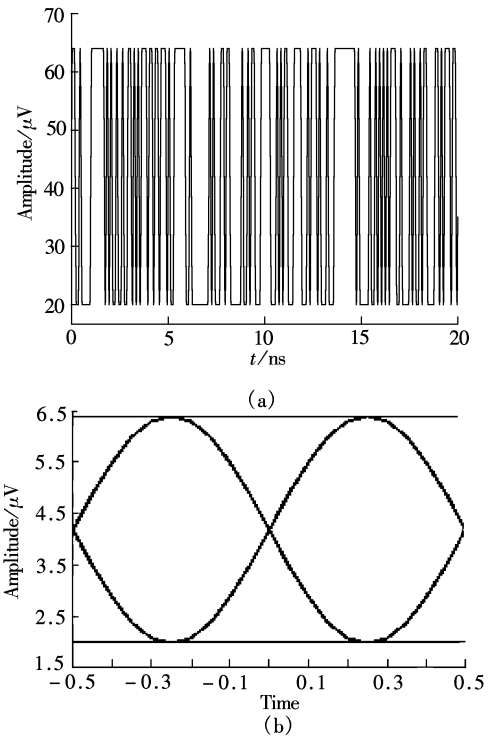

Fig. 7 Waveform and eyediagram of source. (a) Waveform; (b) Eyediagram

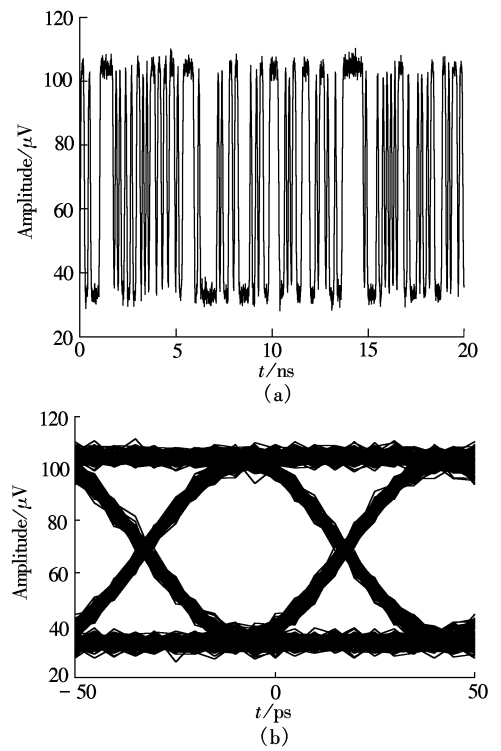

Fig. 8 Output waveform and eyediagram of TIA. (a) Output waveform; (b) Eyediagram

In Fig. 11, two BER simulation results are compared, one for the TIA with high gain, the other for the TIA with low gain, but they have the same overall gain. We can see that in the former case, the output signal of the TIA never drops to the sensitivity of the LA, and thus the sensitivity of the overall receiver is mainly determined by the input-referred noise

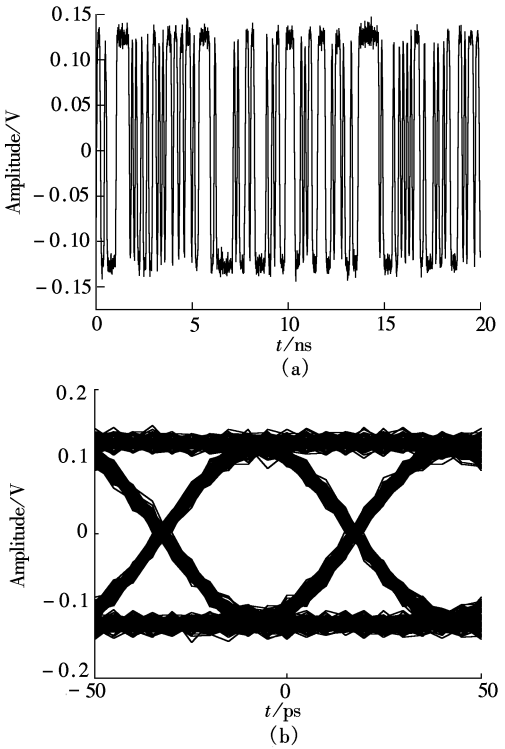

Fig. 9 Output waveform and eyediagram of LA. (a) Output waveform; (b) Eyediagram

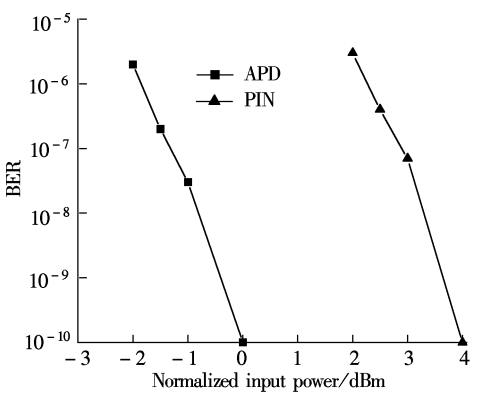

Fig. 10 BER for APD and PIN receivers

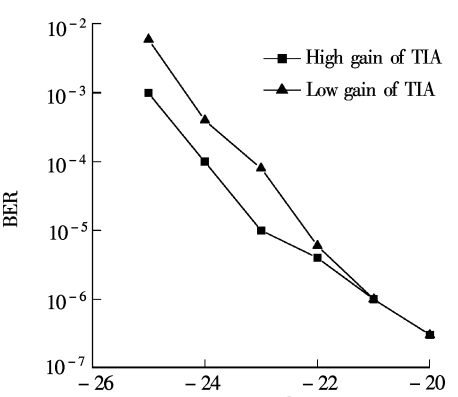

Fig. 11 BER for receivers with high and low gain TIA

of the TIA. However, in the latter case, the output signal drops to near the sensitivity of the LA and the sensitivity of the overall receiver is significantly affected by the input noise of the LA. Additionally, the jitter generated at the output of the LA is increased and may result in an error in the CDR block[9].

Fig. 12 shows the test result for the output of the LA. By comparing the test eyediagram with the simulation eyediagram, the accuracy of the model can be evaluated. The test results show that the variation of the model is below 15%.

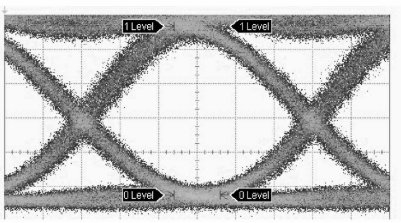

Fig. 12 The test eyediagram of the LA

4 Conclusion

A simple behavior model for the components and the noises of the EPON receiver are presented. The model includes a fiber, a photodetector, a TIA, a LA and a CDR, which are essential parts of the receiver. In this model, the behaviors of each block are modeled. The thermal, shot and dark current noises of the photo detector in the receiver segment are considered. The time-domain models of the TIA and CDR are also considered. The modeling is implemented with C++. The complete electrical circuit model is useful in the analysis of noise in optical communication systems.

References

[1] Mortazy E, Moravvej-Farshi M K. A new model for optical communication systems [J]. *Optical Fiber Technology*, 2005, **11**(1): 69 − 80.

[2] Pepeljugoski P, Golowich S E, Ritger A J, et al. Modeling and simulation of next-generation multimode fiber links [J]. *Journal of Lightwave Technology*, 2003, **21**(5): 1242 − 1255.

[3] Elrefaie A F, Townsend J K, Romeiser M B, et al. Computer simulation of digital lightwave link [J]. *IEEE Journal on Selected Areas in Communications*, 1988, **6**(1): 94 − 105.

[4] Pepeljugoski P K, Kuchta D M, et al. Design of optical communications data link [J]. *IBM Journal of Research and Development*, 2003, **47**(2/3): 223 − 237.

[5] Agrawal Govind P. *Fiber-optic communication systems* [M]. New York: John Wiley & Sons, 2002.

[6] Loyka S L. On the use of Cann's model for nonlinear behavioral-level simulation [J]. *IEEE Transactions on Vehicular Technology*, 2000, **49**(5): 1982 − 1985.

[7] Stojanovic V, Horowitz M. Modeling and analysis of high-speed links [C]//*Proceedings of the IEEE* 2003 *Custom Integrated Circuits Conference*. San Jose, CA, USA, 2003: 589 − 594.

[8] Jeruchim M C, Balaban P, Shanmugan K S. *Simulation of communication systems: modeling, methodology, and techniques* [M]. New York: Kluwer/Plenum, 2000.

[9] Justin R, Craig L. Challenges mark GPON FEC receiver designs [J]. *Lightwave*, 2006, **3**(5): 11 − 14.

以太无源光网络接收机的建模

张 亮 王志功 胡庆生 邓伟杰

(东南大学射频与光电集成电路研究所, 南京 210096)

摘要: 建立了以太无源光网络接受机的行为模型,该模型包括光纤、光电探测器、跨阻放大器、限幅放大器及时钟和数据恢复电路. 模型中各部分都是利用电路结构和行为特性来进行建模的,同时也对它们的噪声和抖动进行了建模,如散粒噪声、热噪声、确定性抖动和随机抖动. 由于使用了行为模型,仿真速度比普通电路模型更快,同时比解析模型更准确. 整个模型用C++语言描述,在 Microsoft Visual C++6.0 中进行实现,并利用蒙特卡洛方法对系统仿真. 最后建立了测试环境对模型进行验证,结果表明仿真结果与实验结果有较好的一致性.

关键词: 以太无源光网络 (EPON); 行为模型; 噪声; 抖动; 时钟数据恢复电路

中图分类号: TN929.11